

Composite Materials for Passive Antiradar Camouflage

CRISTIANA EPURE¹, TEODORA ZECHERU^{2*}, GABRIEL EPURE¹,
CLAUDIU LAZAROAIE¹, OVIDIU IORGA¹, RAZVAN PETRE¹, GABRIELA NITA³,
MIHAIL MUNTEANU¹, DAN STOICA⁴, ALBERT PLOSNITA⁴, VALENTIN RADITOIU⁵

¹Scientific Research Center for CBRN Defence and Ecology, 225 Șos. Olteniței, 041309, Bucharest, Romania

²Armaments Department, 9-11 Drumul Taberei, 061418, Bucharest, Romania

³Military Technical Academy, 39-49 George Coșbuc Blv., 050141, Bucharest, Romania

⁴Center for Test – Evaluation and Scientific Research for Armaments, 16 Str. Aeroportului, 077025, Clinceni, Ilfov, Romania

⁵National Institute for Research & Development in Chemistry and Petrochemistry - ICECHIM, 202 Splaiul Independentei, 060021, Bucharest, Romania

Abstract. *In this study, a new solution for the development of an antiradar camouflage by overlaying several mono-pigment polymeric structures in a composite structure is provided. In this respect, powder materials with antiradar properties (carbon nanotubes, graphite, active charcoal, aluminum trioxide) were embedded in polymeric matrices. The performances of the developed products were tested using an experimental device for the measurement of electromagnetic efficiency within the frequency range from 1 to 18 GHz.*

Keywords: *insertion loss, microwaves, camouflage, carbon*

1. Introduction

Military forces use RADAR systems for air, land or naval surveillance. These RADAR systems usually operate in the range of microwaves (1-12 GHz) [1]. The substances with properties in the field of electromagnetic radiation absorption are called RAMs (Radio absorbing materials) [2], and may include chemicals with regulated honeycomb-like crystal structures [3-10], with magnetic or dielectric properties, able to absorb/attenuate the incident radiation coming from as many directions as possible. The phenomena of microwave absorption take place due to the conversion of the incident radiation beam into heat [11], and the material is more efficient as the level of reflected radiation is lower.

Nevertheless, there is no single material with high absorption rate at all the frequencies. Thus, RAMs can be classified in resonant (for a narrow frequency band) and wide band absorbers. Wide band RAMs are obtained, usually, by mixing different types of resonant materials [12,13]. Further, in order to obtain composite materials, RAMs can be embedded in polymeric matrices [14]. Due to the coating effect, the composite material presents its' best efficiency when employing <1 μ m-particles [10]. RAMs performances are often expressed using the term "shielding effectiveness" or "electromagnetic efficiency", and the measured parameter is the "attenuation" or "insertion loss", which indicates the ratio between the electromagnetic field in a point in space in the absence of the material and the remaining field in the same point in the presence of the same material [6]. The screening efficiency is influenced by the material's structure, its' thickness, the incidence angle and the electromagnetic field's frequency.

Various research papers present methods of obtaining and testing radar absorbing films and several techniques of antiradar camouflage applied in stealth technology, but their disadvantage is represented by the high production costs [15-20].

The aim of this study is to investigate various possibilities of obtaining antiradar camouflage system using environmental-friendly and economically accessible materials. For the development of camouflage materials, different allotropic types of carbon were employed: graphite, active charcoal, fullerenes, and aluminum trioxide (Al₂O₃), the main aim being the widening of the frequency band in

*email: teodora.zecheru@yahoo.com



which the absorption takes place. The substances aforementioned were embedded in a polyurethane elastomer and applied on a support as mono - pigment, both single - and multilayer. The advantages given by such a material are: very low level of toxicity, since the polymeric material employed is free of organic volatile solvents; simplicity and accuracy of application, by using painting classic techniques; adaptability, since the material can be applied in various number- and thickness-wise successive layers; high corrosion resistance, good mechanical, thermal and electrical properties [5, 21-23].

2. Materials and methods

Materials

For the synthesis of the composite material, the following materials were employed as inorganic fillers: ground graphite in different granular sizes (min. 95% wt purity, Reactivul), active charcoal (min. 98% wt purity, CCSACBRNE), carbon nanotubes (min. 95% wt purity, Cheap Tubes), Al₂O₃ (min. 99.5% wt purity) and toluene (min. 99.8% wt purity) from Merck, solvent-free castor oil-based hydroxyl functionalised acrylic polyol (NUPLEX[®]), solvent-free solvent-free diphenylmethane-based aromatic polyisocyanate (COVESTRO[®]).

Graphite was prepared by grinding in a ceramic ball mill during 6 h, then by sorting by granulometric size sorting, using a vibrating sieve shaker. Only the fractions remained on the 45 µm and 38 µm sieves and the residual from the plate were selected.

Method for the synthesis of the composite materials

In order to fill the pores in charcoal and to untangle and reorient the fibers in the nanotubes case, the active charcoal and the carbon nanotubes were wetted with organic solvent before incorporating them in polyol (1:4 (w:w) filler:toluene).

In order to obtain the RAM composites, the following steps were pursued at room temperature: firstly, the inorganic fillers were weighed and mixed in liquid phase; secondly, component 1 (C1) was obtained by dispersing the powder materials in polyol as C1A: 80:20 (w:w) polyol:filler (graphite, Al₂O₃) and C1B: 98:2 (w:w) polyol:filler (active charcoal, carbon nanotubes), using an ultrasonic mixer, until a 50 µm-particle size was reached. The particle size was measured with a grindometer (accordingly to SR EN ISO 1524:2013).

In order to create the chemical crosslinking for the coating to be applied on a support, component 2 (C2), the polyisocyanate, was added to C1 in the following ratios: 125:50 (w:w) C1A:C2 and 100:50 (w:w) C1B:C2. C2 was slowly added to C1 during 15 min before application on the support.

Further on, to obtain the samples, the binder polyol-polyisocyanate from the composite material was poured in 250x250x7 mm molds. The composite material for the tests was applied on samples with the mentioned dimensions, using classic painting method: by spraying, rolling or brushing. The obtained composite materials were applied on samples in single or multi-layer. In Table 1 is presented the configuration of the tested samples, where: PU is the polyurethane support; C.a. – the film containing active charcoal with grain size $d < 63 \mu\text{m}$; G45 – the film containing graphite with grain size $45 < d < 63 \mu\text{m}$; G38 – the film containing graphite with grain size $38 < d < 45 \mu\text{m}$; GT – the film containing graphite with the grain size $d < 38 \mu\text{m}$ (collected from the plate); Al₂O₃ – the film containing the corresponding oxide; MWCNT (multi wall carbon nanotubes) – the film containing carbon nanotubes; x – one layer; xx – two layers (the layer thickness of min. 50 µm).

Table 1. Composition of the tested samples

Sample number/ Raw material	PU	C.a.	G45	G38	GT	Al ₂ O ₃	MWCNT
1	X						
2	X	x					
3	X		x				
4	X			x			
5	X				x		

6	X					x	
7	X						x
8	X			x			x
9	X						xx
10	X			x		x	x

Characterization

In order to evaluate the shape and the spatial distribution of the particles, a scanning electronic microscope (SEM) with thermo-ionic emission with wolfram filament for the electron beam VEGA II LMU – Tescan was used. The SEM analysis was performed in high vacuum conditions, 6×10^{-7} Torr, with the secondary electrons detector (SE), resolution view, emission voltage 30 kV or 5 kV versus sample type and magnification required. In order to determine the performances, a testing setup was made inside an anechoic chamber, illustrated in Figure 1.

A generator within the frequency range 9 kHz to 20 GHz was employed as high frequency signal source, while the receptor (spectrum analyzer and amplifier) scanned within the range 2 Hz to 26 GHz; the operation mode: receptor/spectrum analyzer/vector analyzer. For both emission and reception signals, antennas were set for frequencies between 1 GHz and 18 GHz. The measurements were made at different frequencies from 1 to 18 GHz. For each frequency, the emitted power (measured by the generator) and the reflected power (measured by the receptor) were recorded.

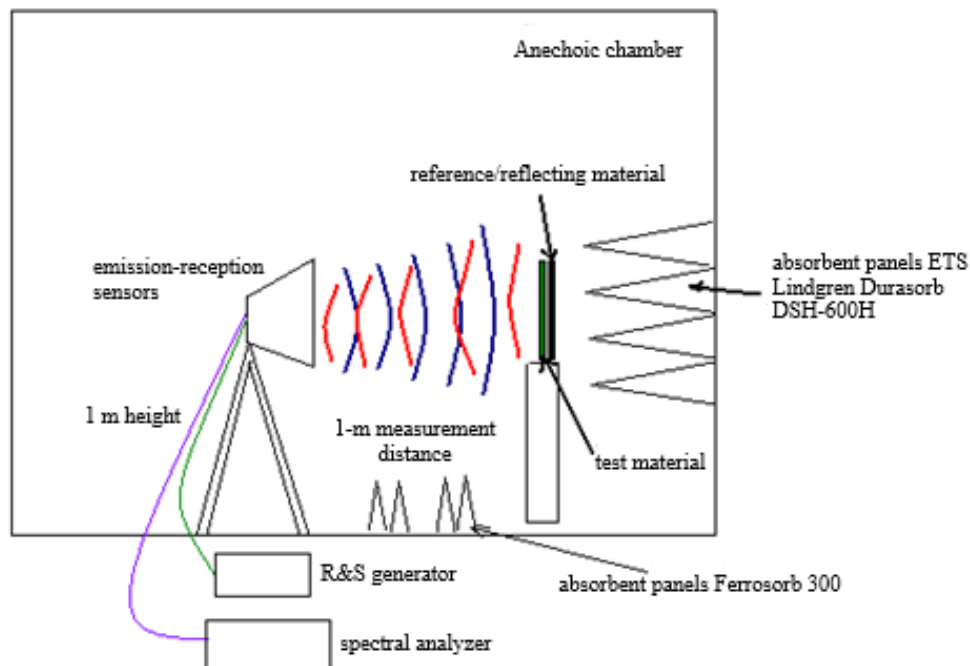


Figure 1. Setup for the measurement of the materials’ electromagnetic absorption potential

As reference, a nontransparent metallic plate with conductive properties was placed behind the samples, having the role to reflect all the incident radiations that were not absorbed by the tested material, so that the obtained results could be compared.

3. Results and discussions

Regarding the comparative evaluation of the raw materials, as shown in the images on the different varieties of graphite (Figures 2-4), the graphite is a planar, layered structure. In the atomic plane, the carbon atoms are arranged in a honeycomb-like structure.

Three out of the four valence electrons are part of covalent bonds, while the fourth is free to move, giving to graphite both conductive properties and radiation absorption capacity, stopping the incident radiation to be reflected back to the generator.

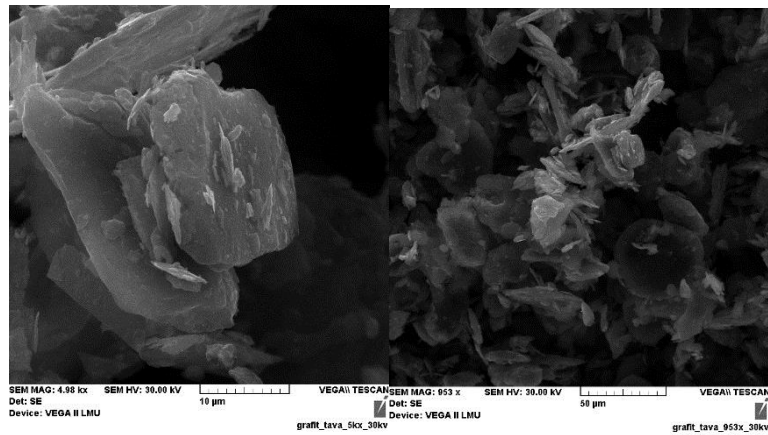


Figure 2. GT graphite morphostructure

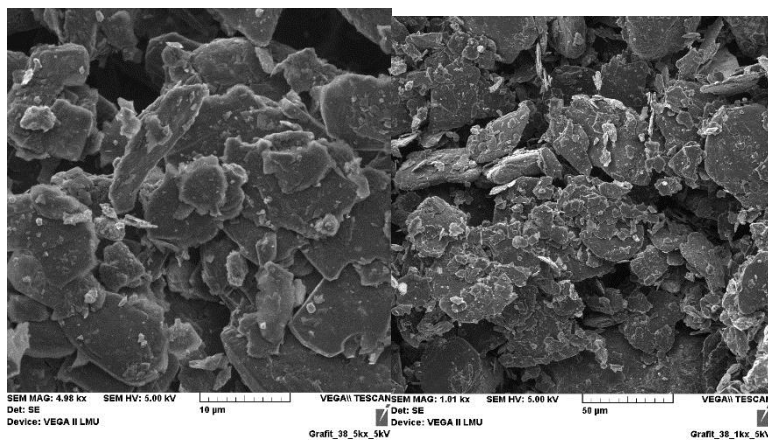


Figure 3. G38 graphite morphostructure

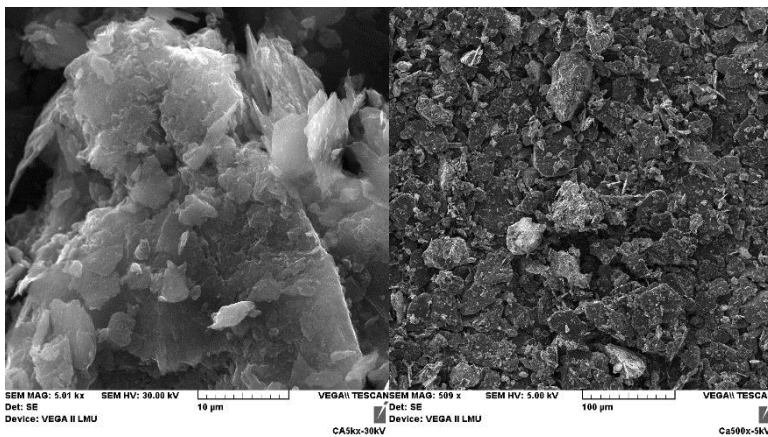


Figure 4. G45 graphite morphostructure

The active charcoal is a type of graphite processed as to expose micrometric pores, in order to increase the adsorption surface. Structurally-wise, the active charcoal is represented by a conglomerate of graphite microcrystals with ca. 20x20 Å dimensions [24]. The morphostructure of the used active charcoal is illustrated in Figure 5.

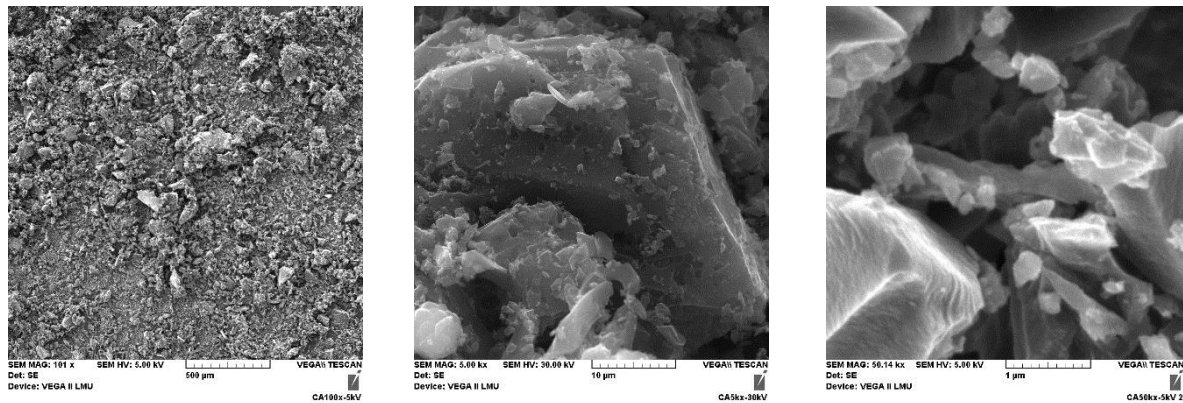


Figure 5. Active charcoal morphostructure

The MWCNT used have a multi-stratified structure (Russian doll) [25]. Each nanotube comprises two or more concentric tubes of different diameters, which can have different structures, generating a wide variety of possible arrangements. The simplest arrangement is obtained when the concentric layers have an identical structure, but different diameters. In normal conditions, they are bundled together (Figure 6).

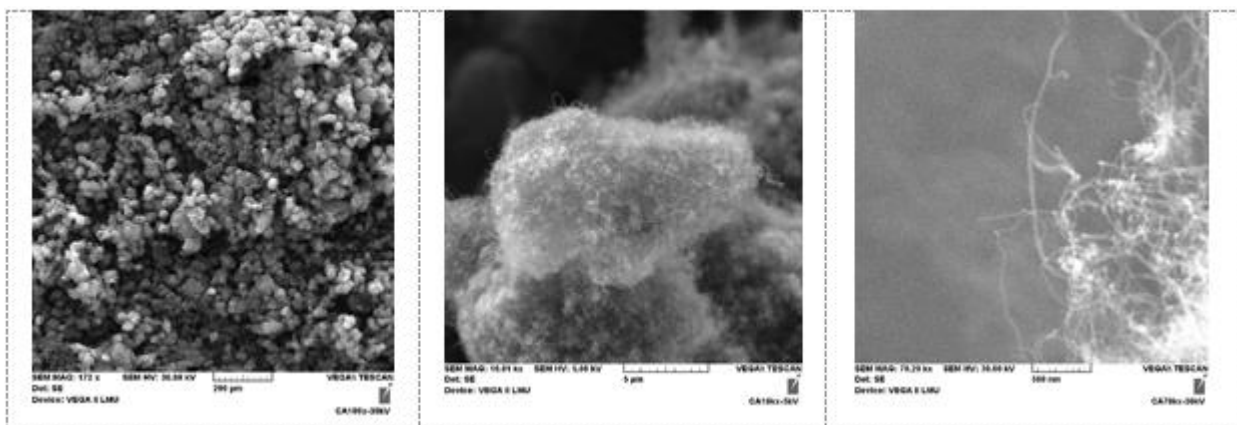


Figure 6. MWCNT morphostructure

Each material obtained during the study presents an insertion loss in a certain frequency band, while this band varies from one material to another. In Table 2 there are illustrated the properties of the synthesized RAMs. As one may notice, not all the materials are efficient in antiradar camouflage.

The highest insertion losses were obtained with carbon nanotubes, at frequencies between 5 and 17 GHz, with G38 graphite at frequencies between 4-5 GHz and 16 GHz, with active charcoal between 4-5 GHz, and with Al₂O₃ at 16 GHz. Based on these experimental results, several layers were applied in order to create the widest frequency band efficiency.

Table 2. Insertion loss versus electromagnetic radiation frequency for mono-layer samples

Frequency (GHz)	Sample / Insertion loss					
	2 (PU/C.a.)	3 (PU/G45)	4 (PU/G38)	5 (PU/GT)	6 (PU/Al ₂ O ₃)	7 (PU/MWCNT)
1	2.0	1.8	1.3	1.2	1.3	1.6
2	1.1	0.5	0.6	0.1	0.3	3.6
3	2.2	1.3	2.7	1.8	0.8	3.2
4	5.0	-	5.9	3.5	2.7	3.8

5	5.0	-	7.0	3.6	2.5	5.1
6	1.0	0.1	0.2	0.5	1.0	6.5
7	1.6	3.8	3.8	2.4	4.3	6.2
8	0.7	3.4	4.2	2.8	4.0	8.7
9	0.8	2.3	3.8	2.9	3.3	8.2
10	3.8	1.2	0.4	1.3	3.9	7.2
11	1.9	0.4	0.5	2.2	3.7	6.9
12	2.0	3.1	3.3	4.2	4.0	4.3
13	3.1	2.5	2.3	1.2	2.8	5.3
14	1.6	1.4	1.8	1.3	4.4	7.3
15	1.0	1.6	0.4	1.2	2.6	3.1
16	2.6	3.0	5.4	4.6	5.2	2.8
17	1.5	3.1	2.8	3.6	0.9	13.6
18	3.7	2.8	2.7	3.0	2.7	0.6

For this purpose, the selected materials were the MWCNT, the graphite G38 and Al₂O₃. The results, presented in Table 3, revealed that a higher concentration of MWCNT (the thickness of the layer) provides a higher insertion loss (sample 7 versus sample 9). The multi-layer coating made of successive layers of graphite, MWCNT and Al₂O₃ generate the highest values of insertion loss on the entire spectrum of tested frequencies (no attenuation below 4 dB), while the neat polyurethane binder does not present antiradar properties.

Table 3. Insertion loss for different incident radiation frequencies in the case of the multi-layer samples

Frequency, GHz	Sample/Insertion loss				
	1 (PU)	7 (PU/MWCNT)	8 (PU/G38/MWCNT)	9 (PU/MWCNT/MWCNT)	10 (PU/Al ₂ O ₃ /G38/MWCNT)
1	1.1	1.6	3.8	1.9	4.0
2	2.6	3.6	5.5	5.7	6.0
3	1.2	3.2	5.6	4.9	5.3
4	1.8	3.8	7.2	7.0	6.9
5	1.4	5.1	7.2	7.4	7.3
6	3.0	6.5	9.8	8.7	7.9
7	0.1	6.2	7.3	8.7	9.6
8	2.3	8.7	5.8	12.4	14.0
9	3.3	8.2	7.6	14.3	14.3
10	2.2	7.2	6.3	13.3	12.0
11	2.3	6.9	7.2	8.9	8.9
12	2.3	4.3	9.6	6.2	6.9
13	1.4	5.3	7.1	4.3	7.2
14	1.9	7.3	12.3	10.5	10.8
15	0.8	3.1	12.4	6.7	4.5
16	2.1	2.8	14.9	8.8	10.7
17	0.1	13.6	5.8	4.5	10.4
18	1.5	0.6	2.3	0.9	4.1

4. Conclusions

The aim of this paper was to study the possibility of developing composite materials for antiradar camouflage by embedding RAMs in polymeric matrices (bicomponent polyurethane binder) and applying them as paint-like layers. It was observed that the main performance parameter of RAMs was based on the symmetrical, multi-stratified honeycomb-like crystalline structure. Amorphous substances, such as polymers, do not possess such qualities. Thus, to obtain a wide absorbed frequency band, the composite material must be a multi-layer structure, with several mono-pigment layers applied on the support. The absorption rate is heavily influenced by the thickness of the layers. By choosing an appropriate layer thickness, the width of the absorption band can be considerably enlarged, both in the case of frontal and oblique incident radiation. From the tested RAMs, the graphite with a grain size $d < 38 \mu\text{m}$, the MWCNT and the Al_2O_3 were the elements that influenced in a positive way the insertion loss, each one in a different frequency band. To cover a wider range of microwave frequencies, a multi-layer antiradar structure was developed, each layer containing one of the aforementioned absorbents. Insertion losses above 4 dB were obtained, for frequencies between 1 to 18 GHz, up to 14 dB in X band, which conducts to the conclusion that the materials obtained may be further tested for implementation as antiradar camouflage materials.

Acknowledgements. This work was supported by a grant of the Romanian Ministry of Research and Innovation, PCCDI-UEFISCDI, project no. PN-III-P1-1.2-PCCDI-2017-0395 (Research Contract No. 70PCCDI/2018) Contingency of CBRN hazards and improvement of national security resources SECURE-NET – PC5 - Passive multispectral camouflage systems based on chromogenic-polymeric organic-inorganic hybrid structures – MULTICAM.

References

- 1.VINOY, K.J., JHA, R.M., Radar absorbing materials: from theory to design and characterization, Springer US, 1996.
- 2.XIANG, Z., SONG, Y., XIONG, J., PAN, Z., WANG, X., LIU, L., LIU, R., YANG, H., LU, W., Carbon, **142**, 2019, p. 20-31.
- 3.WANG, C., MURUGADOSS, V., KONG, J., HE, Z., MAI, X., SHAO, Q., CHEN, Y., GUO, L., LIU, C., ANGAIAH, S., GUO, Z., Carbon, **140**, 2018, p. 696-733.
- 4.SINGH, A.K., SHISHKIN, A., KOPPEL, T., GUPTA, N., Compos. Part B-Eng., **149**, 2018, p. 188-197.
- 5.LIU, Y., SONG, D., WU, C., LENG, J., Compos. Part B-Eng., **63**, 2014, p. 34-40.
- 6.ZHANG, L., WANG, L.B., SEE, K.Y., MA, J., J. Mater. Sci., **48**, no. 21, 2013, p. 7757-7763.
- 7.PEGEL, S., PÖTSCHKE, P., PETZOLD, G., ALIG, I., DUDKIN, S.M., LELLINGER, D., Polymer **49**, no. 4, 2008, p. 974-984.
- 8.CHUNG, D.D.L., Carbon, **39**, no. 2, 2001, p. 279-285.
- 9.CLARK, D.E., FOLZ, D.C., WEST, J.K., Mater. Sci. Eng. A, **287**, no. 2, 2000, p. 153-158.
- 10.RUCK, G.T., BARRICK, D.E., STUART, W.D., KIRCHBAUM, C.K., Radar cross section handbook, vol. 1, Plenum Press, New York, 1970.
- 11.MICHELI, D., VRICELLA, A., PASTORE, R., MARCHETTI, M., Carbon, **77**, 2014, p. 756-774.
- 12.BARNA, E., BOMMER, B., KÜRSTEINER, J., VITAL, A.V., TRZEBIATOWSKI, O., KOCH, W., SCHMID, B., GRAULE, T., Compos. Part A Appl. Sci. Manuf., **36**, no. 4, 2005, p. 473-480.
- 13.BOURZAC, K., Nano paint could make airplane invisible to radar, Technology Review. MIT, 2011.
- 14.GUPTA, T.K., SINGH, B.P., DHAKATE, S.R., SINGH, V.N., MATHUR, R.B., J. Mater. Chem. A, **1**, no. 32, 2013, p. 9138-9149.
- 15.SCHMID, E.V., Exterior durability of organic coatings, FMJ International, Surrey, 1988.
- 16.BOKOBZA, L., Spectroscopic Techniques for the Characterization of Polymer Nanocomposites: A Review. Polymers (Basel), **10**, no. 1, 2018, p. 7-27.



17. VISAKH, P.M., MARKOVIC, G., PASQUINI, D., Recent Developments in Polymer Macro, Micro and Nano Blends – Preparation and Characterisation, Woodhead Publishing, 2017.
18. FRIEDRICH, K., BREUER, U., Multifunctionality of Polymer Composites – Challenges and New Solutions, William Andrew Ed., 2015.
19. IWAMARUA, T., KATSUMATA, H., UEKUSA, S., OYAYAGI, H., ISHIMURA, T., MIYAKOSHI, T., Physics Procedia, **23**, 2012, p. 69-72.
20. MOURITZ, A.P., Introduction to Aerospace Materials, Woodhead Publishing, 2012, p. 268-302.
21. GUPTA, T.K., SINGH, B.P., DHAKATE, S.R., SINGH, V.N., MATHUR, R.B., J. Mater. Chem. A, **1**, no. 32, 2013, p. 9138-9149.
22. SCHMID, E.V., Exterior durability of organic coatings, FMJ International, Surrey, 1988.
23. ROȘU, D., ROȘU, L., *Mater. Plast.*, **47**(4), 2010, 399-404.
24. NAKAYAMA, A., SUZUKI, K., ENOKI, T., Bull. Chem. Soc. Jpn., **69**, no. 2, 1996, p. 333-339.
25. ***www.cheaptubes.com/product-category/multi-walled-carbon-nanotubes (accessed on 20 December 2019).

Manuscript received: 02.02.2020